Tunnel ionization of molecules and orbital imaging

Murray, Ryan; Spanner, Michael; Patchkovskii, Serguei; Ivanov, Misha Yu

Publisher's version / Version de l'éditeur:
https://doi.org/10.1103/PhysRevLett.106.173001
Physical Review Letters, 106, 17, pp. 173001-1-173001-4, 2011-04-28

Tunnel Ionization of Molecules and Orbital Imaging

Ryan Murray,[1,2] Michael Spanner,[3] Serguei Patchkovskii,[4,*] and Misha Yu. Ivanov[2]

[1]University of Waterloo, Waterloo ON, N2L 3G1, Canada
[2]Department of Physics, Imperial College London, South Kensington Campus, SW7 2AZ London, United Kingdom
[3]National Research Council of Canada, 100 Sussex Drive, Ottawa, ON, K2A 0R6, Canada
[4]Max-Born Institute for Nonlinear Optics and Short Pulse Spectroscopy, Max-Born-Strasse 2A, D-12489 Berlin, Germany

(Received 6 December 2010; published 28 April 2011)

We study whether tunnel ionization of aligned molecules can be used to map out the electronic structure of the ionizing orbitals. We show that the common view, which associates tunnel ionization rates with the electronic density profile of the ionizing orbital, is not always correct. Using the example of tunnel ionization from the CO_2 molecule, we show how and why the angular structure of the alignment-dependent ionization rate moves with increasing the strength of the electric field. These modifications reflect a general trend for molecules.

DOI: 10.1103/PhysRevLett.106.173001 PACS numbers: 33.80.Rv, 42.50.Hz

Ionization of atoms or molecules is at the core of nearly every process in strong laser fields, from high harmonic generation to correlated multiple ionization to laser induced electron diffraction and holography [1]. The ability to align molecules [2] allows one to measure their ionization as a function of molecular alignment relative to the polarization of intense infrared laser field. It has recently been argued (see, e.g., [3,4]) that these measurements of the ionization rates map out the geometry of the ionizing orbital. Intuitively, the rate is expected to (i) minimize when the ionizing laser field is aligned with the nodal plane of the molecular orbital and (ii) maximize when the laser field is lined up with the most spatially extended component of the orbital.

However, in some cases experiment disagrees with this intuitive picture. A striking example is strong-field ionization of the CO_2 molecule. Intuitively, one expects its tunnel ionization rate to peak when the field is aligned at about 30° relative to the molecular axis, i.e., along the most spatially extended component of the highest occupied molecular orbital. The tunneling theory MO-ADK [5] indeed predicts this result (e.g., [6,7]), as well as the new tunneling approach developed in [8]. However, the experiment [9] observed sharply peaked ionization at about 45°. The standard tunneling theory does not reproduce these results [5–8,10,11], while the numerical solutions of the time-dependent Schrödinger equation fit the surprising positions of the peaks [10,12] well. The physics responsible for this effect is a subject of hot debate (see, e.g., [7,10,11,13]), including the possible contribution of multiphoton resonances ignored in the tunneling picture [10], or multiple ionic states (multiple orbitals) [13]. The extreme sharpness of the peaks in [9], not observed in [14] and questioned in [7,10], might indeed be related to the artifacts in the deconvolution procedure (see [10]), which is required to extract the ionization rates when dealing with imperfect molecular alignment. However, the rotation of the ionization peaks to about 45° was confirmed [15].

Based on our analysis below, we can infer that this surprising observation is not special to CO_2 and reflects a general trend in polyatomic molecules, which does not require the contribution of multiple ionizing orbitals or multiphoton resonances (even though these may and will play a role in specific cases [13]). Our analysis builds on the approach of Ref. [16], extending the work of Popov and co-workers [17]. It shows the interplay of coordinate- and momentum-space properties of the ionizing orbital in tunnel ionization. The relative role of the coordinate-space versus momentum-space features changes as one changes the strength of the ionizing field, with the momentum-space features becoming more important at higher field strengths. Figure 1 shows our analytical predictions for the example of a CO_2 molecule, demonstrating the rotation of the maxima from about 30° to about 45° with increasing field strength.

Rotation of the alignment-dependent ionization rates with field strength has not been obtained in the previous tunneling approaches. Since our analytical expressions include the standard MO-ADK tunneling theory [5] as a limiting case, they show how and why deviations arise at high field strengths.

Let z be the direction of the electric field F that induces tunnel ionization. The ionization rate is given by the total current through the plane orthogonal to z:

$$\Gamma = \frac{1}{2}\int dxdy\Psi^*(x, y, z)\hat{p}_z(z)\Psi(x, y, z) + \text{c.c.}, \qquad (1)$$

where atomic units $e = m_e = \hbar = 1$ are used, $\hat{p}_z$ is the electron momentum operator orthogonal to the x-y plane, and Ψ is the wave function of the tunneling electron beyond the tunnel exit. For multielectron systems the role of Ψ is taken by the Dyson orbital, i.e., the overlap between the initial N-electron wave function of the neutral and the final $N-1$ electron wave function of the ion. The continuity equation ensures that the total current is z independent after the tunneling electron exits the barrier.

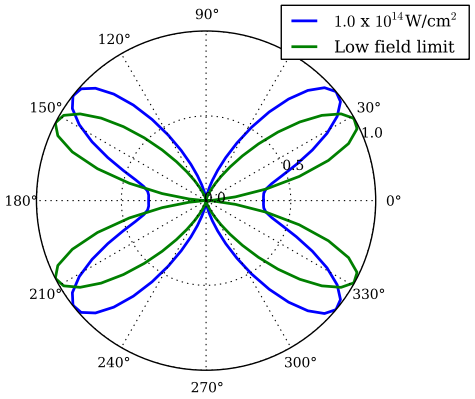

FIG. 1 (color online). Tunnel ionization rate of a CO_2 molecule for low and high strength of the ionizing dc electric field. Only the dimensionless alignment-dependent factor is shown.

To calculate the rate, we pick a point z_0 between the entrance $z_{\rm in}$ and the exit $z_{\rm ex}$ from the tunneling barrier, where we assume the wave function to be known (Fig. 2). In practice, the required Dyson orbital is found at a plane $z = z_0$ using quantum chemistry methods (see below). Following Ref. [16], we rewrite $\Psi(x, y, z_0)$ as

$$\Phi(p_x, p_y, z_0) = \frac{1}{2\pi} \int dx \int dy e^{-ixp_x - iyp_y} \Psi(x, y, z_0). \quad (2)$$

$\Phi(p_x, p_y, z_0)e^{ixp_x + iyp_y}$ can be effectively propagated under the barrier using the semiclassical (WKB) method, assuming small deviations of tunneling trajectories from the z axis and treating core potential in the eikonal approximation. Then, at a point z near $z_{\rm ex} \approx I_p/F$ (I_p is the ionization potential) we find [16]

$$\Phi(p_x, p_y, z) \simeq \Phi(p_x, p_y, z_0) \sqrt{\frac{\kappa}{|p_z(z)|}} \times \exp\left[- \int_{z_0}^{z} p_z(z')dz' - \frac{(p_x^2 + p_y^2)\tau_T}{2} \right], \quad (3)$$

where $\kappa = \sqrt{2I_p}$ and $\tau_T \simeq \kappa/F$. Going back to the coordinate space yields

$$\Psi(x, y, z) \simeq \sqrt{\frac{\kappa}{|p_z(z)|}} e^{-\int_{z_0}^{z} p_z(z')dz'} \frac{1}{2\pi} \times \int dp_x dp_y e^{-ixp_x - iyp_y} \Phi(p_x, p_y, z_0) e^{-(1/2)p_\perp^2 \tau_T}, \quad (4)$$

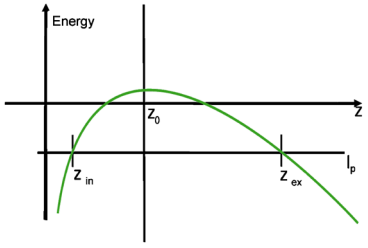

FIG. 2 (color online). Schematic of tunneling, with $z_{\rm in}$ and $z_{\rm ex}$ the entrance and the exit points and z_0 is the matching point.

with $p_\perp^2 \equiv p_x^2 + p_y^2$. Equation (4) can now be substituted into Eq. (1). Note that the factor $1/\sqrt{|p_z(z)|}$ cancels in the tunneling current, allowing one to set $z = z_{\rm ex}$ in Eq. (1).

Equation (4) shows how tunneling combines the coordinate and momentum-space characteristics of the orbital. The z_0 dependence of $\Phi(p_x, p_y, z_0)$ means that tunneling benefits from orbital's extension in the coordinate space along the electric field. At the same time, the integral shows filtering in the momentum space, which tends to cut contributions of high momentum components, discouraging tunneling at large angles relative to the electric field. The filter $G(p_\perp) = \exp[-p_\perp^2 \tau_T/2]$ becomes less severe as $\tau_T = \kappa/F$ decreases with increasing F, allowing higher momentum components of the orbital in the x-y plane to contribute to ionization. The interplay of these two features, together with the transmission amplitude $\exp[-\int p_z(z')dz']$ which incorporates the shape of the barrier, determines alignment dependence of the ionization rate and how this dependence changes with the field; see Fig. 1.

To feel how these features play out, we approximate $\Psi(x, y, z_0)$ for $z_0 \gg z_{\rm in}$ as

$$\Psi(x, y, z_0) \simeq C_\kappa \kappa^{3/2} \frac{e^{-\kappa r_0}}{\kappa r_0} (\kappa r_0)^{Q/\kappa} f_M(\theta_M, \phi_M). \quad (5)$$

Here the spherical angles θ_M and ϕ_M refer to the molecular frame and $z_0 \equiv r_0 \cos\theta_M$. The function f_M (in the molecular frame) incorporates the geometry of the orbital which, in turn, reflects the shape of the binding potential. Deviations from the single-center Coulomb potential, very significant near the core, are responsible for how f_M looks in the asymptotic region $z_0 \gg z_{\rm in}$. The radial asymptotic behavior corresponds to the Coulombic tail $-Q/r$ of the potential.

First, we transform $f_M(\theta_M, \phi_M)$ from the molecular frame to $f_L(\theta, \phi; \theta_L)$ in the lab frame, which requires rotation by θ_L in the x-z plane. Second, we calculate the Fourier transform of $G(p_\perp) \times \Phi(p_x, p_y, z_0)$ in Eq. (4), directly in the coordinate space using the convolution theorem. Finally, we calculate the tunneling current.

Substituting Eq. (5) into Eqs. (4) and (1), and calculating the tunneling integral between z_0 and z for the potential $-Q/r$ following [17] (i.e., using the eikonal approximation to match the asymptotic form of the radial wave function), we obtain

$$\Gamma = \Gamma_{A,s} R(\theta_L) = \left[\frac{\pi}{\tau_T} C_\kappa^2 e^{-(2\kappa^3/3F)} \left(\frac{2\kappa^3}{F} \right)^{2Q/\kappa} \right] R(\theta_L). \quad (6)$$

The first term, $\Gamma_{A,s}$, is the standard tunneling rate for an atomic s orbital with no angular structure. The second term, $R(\theta_L)$, incorporates all aspects of the orbital geometry, including the interference of the tunneling currents coming from the different lobes of the orbital:

$$R(\theta_L) = \frac{1}{R^{(0)}} \frac{1}{\pi\tau_T} \times \int_0^\infty \rho d\rho e^{-\rho^2/\tau_T} \int_0^{2\pi} d\phi |\tilde{f}_L(\rho, \phi; \theta_L)|^2. \quad (7)$$

Here $\rho = \rho(\theta) = r_0 \sin\theta$ and $\tilde{f}_L$ comes from the Fourier integral in Eq. (4), here written via the convolution:

$$\tilde{f}_L(\rho, \phi; \theta_L) = \int_0^\infty \rho' d\rho' e^{-\rho'^2/2\tau_T} e^{-\kappa\rho'^2/2z_0} \frac{1}{2\pi} \times \int_0^{2\pi} d\phi' e^{\rho\rho'\cos(\phi-\phi')/\tau_T} f_L(\theta', \phi'; \theta_L). \tag{8}$$

The normalization factor $R^{(0)}$ is obtained by setting $f_L = 1$ (i.e., atomic s orbital).

Let us focus on the orbitals with Σ and Π symmetry. The x-z plane of the lab frame is defined by the molecular axis Z_M and the electric field (the lab axis z). The Π_y orbital has a nodal plane and its ionization is suppressed for all angles. For Σ and Π_x orbitals $f_M(\theta_M, \phi_M) = F(\cos\theta_M, \sin\theta_M \cos\phi_M)$ and for the Π_y orbital $\sin\theta_M \cos\phi_M$ is replaced with $\sin\theta_M \sin\phi_M$. For Σ orbitals the term $\sin\theta_M$ is absent, while for Π_x orbitals $F = f(\cos\theta_M)\sin\theta_M \cos\phi_M$. We will use the notation $F(u, v)$, where $u = \cos\theta_M$ and $v = \sin\theta_M \cos\phi_M$. The frame transformation is standard: $\cos\theta_M \to \cos\theta_L \cos\theta - \sin\theta_L \sin\theta \cos\phi$; $\sin\theta_M \cos\phi_M \to \cos\theta_L \sin\theta \cos\phi + \sin\theta_L \cos\theta$ with θ and ϕ angles in the lab frame, and θ_L is the angle between the molecular axis and the electric field. Substituting these expressions into $F(u, v)$, we evaluate required integrals expanding $F(u, v)$ in Taylor series with respect to θ, up to the second order. The result is

$$R(\theta_L, z_0) \simeq \left[F_0 - F_2 \frac{1}{2}\theta_T^2(z_0) + F_3 \frac{1}{4}\theta_T^2(z_0)\right]^2 + \frac{1}{2\tau_T}\left(F_1 \frac{1}{2}\theta_T^2(z_0) z_0\right)^2, \tag{9}$$

where $\theta_T(z_0) = \sqrt{2}/\sqrt{(\kappa + z_0/\tau_T)z_0}$ is the characteristic angular width of the tunneling wave function at the matching point z_0. Here $F_0 = F(\cos\theta_L, \sin\theta_L)$ describes the angular function itself, while the rest of F_k are related to the derivatives in the direction orthogonal to z, calculated at $u = \cos\theta_L$ and $v = \sin\theta_L$:

$$\begin{aligned} F_1 &= F_v \cos\theta_L - F_u \sin\theta_L, \\ F_2 &= F_u \cos\theta_L + F_v \sin\theta_L, \\ F_3 &= F_{vv}\cos^2\theta_L + F_{uu}\sin^2\theta_L - F_{uv}\sin 2\theta_L. \end{aligned} \tag{10}$$

We can now analyze the interplay of the coordinate-space and momentum-space features of the ionizing orbital in detail. The tunneling angle θ_T is small, and hence the terms proportional to $F_{1,2,3}$ would typically be neglected. In this approximation, $R(\theta_L) \simeq F_0^2 \equiv F^2(\cos\theta_L, \sin\theta_L)$ and the alignment-dependent rate does indeed map out the orbital. The neglected terms are always important near the nodal planes of the orbital, where $F_0 = 0$. There, the dominant correction comes from the F_1 term, yielding

$$R(\theta_L) \simeq F_0^2 + \frac{1}{2\tau_T \kappa^2} F_1^2. \tag{11}$$

Here the dependence of $R(\theta_L, z_0)$ on the matching point is removed, as is common in the asymptotic tunneling theories, by setting $z_0/\kappa\tau_T \ll 1$. Applying Eq. (11) to the atomic s and p orbitals leads to results identical with standard expressions [17]. Equation (11) is nothing but the compact form of the tunneling theory for molecules (MO-ADK), but written without using the expansion of the ionizing orbital into the spherical basis.

This simple picture breaks down for the fields of a few volts per angstrom, which are typical in many practical situations. Under such conditions the F_1 term becomes important in a broader range of angles, not only where $F_0 = 0$. The terms proportional to F_2 and F_3 are also no longer negligible. Formally, the requirement $z_{\rm in} \ll z_0 \ll z_{\rm ex}$ can no longer be met, and the z_0 dependence in Eq. (9) should be handled differently. We follow the angle $\theta_T(z_0)$ adiabatically to the exit from the barrier, substituting $z_0 \to z_{\rm ex}$ in $\theta_T(z_0)$: $\theta_T(z_{\rm ex}) = \sqrt{2/(\kappa + z_{\rm ex}/\tau_T)z_{\rm ex}}$, with $z_{\rm ex} \approx I_p/F$ and $\tau_T \approx \kappa/F$. The corresponding expression for $R(\theta_L)$ is

$$R(\theta_L) = R(\theta_L, z_{\rm ex}) \simeq \left[F_0 - \frac{\theta_T^2(z_{\rm ex})}{2} F_2 + \frac{\theta_T^2(z_{\rm ex})}{4} F_3\right]^2 + \frac{1}{2\tau_T} \frac{1}{(\kappa + z_{\rm ex}/\tau_T)^2} F_1^2. \tag{12}$$

We use $F(\cos\theta_M, \sin\theta_M \cos\phi_M)$ from Ref. [18]):

$$F(\cos\theta_M, \sin\theta_M \cos\phi_M) = \cosh(\lambda \cos\theta_M)(1 + c^2\cos^2\theta) \times (\cos\theta_M)^n (\sin\theta_M \cos\phi_M)^m, \tag{13}$$

where for Σ orbitals $m = 0$ and for Π_x orbitals $m = 1$. For distances $r_0 = 6$–8 a.u. from the origin the parameters in Eq. (13) are $\lambda = 2.5$, $n = 1$, $m = 1$, $c = 0$, $C_\kappa = 0.66$, for the Dyson orbital corresponding to the ionization from the CO_2 ground state to the CO_2^+ ground state. The Dyson orbital was evaluated from the complete active space self-consistent field (CASSCF) wave functions [19] using the GAMESS code with the modified aug-cc-pV5Z basis [20], where the $L = 5$ functions were removed and 2 sets each of uncontracted even-tempered S, P, and D functions, with orbital exponents scaled by factors 0.4 and 0.16 relative to the most diffuse functions of the same symmetry in the original basis set, were added. The CASSCF calculations use 16 (neutral) or 15 (cation) active electrons in 11 orbitals. The $(3\times)$ $1s$ atomic orbitals were not included.

The resulting factor $R(\theta_L)$, calculated using Eq. (12) (for a static field), is compared in Fig. 3(b) with the results of *ab initio* calculations for various field strengths. In order to facilitate comparison with the static field analytical results, for the numerical simulations we use a quasistatic field with smooth turn-on and turn-off: $F(t) = F_0 \sin^2(\frac{\omega t}{\sqrt{2}})$ for $0 < t < \tau_{\rm on}$ and $F(t) = 0$ otherwise, with $\tau_{\rm on} = \pi/\omega\sqrt{2}$ and $\omega = 0.0285$ a.u. Near its peak this field mimics a half-cycle pulse of 1600 nm light. The propagation equations of Ref. [21] were integrated in time using the leapfrog method. The ionization yield was computed by monitoring

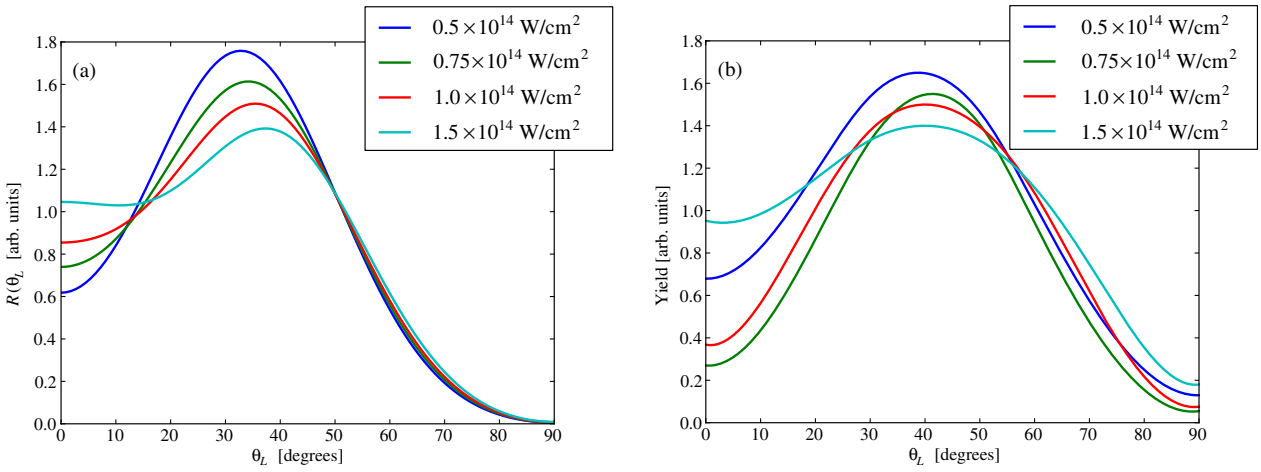

FIG. 3 (color online). Ionization of a CO_2 molecule into the ground electronic state of the cation at the equilibrium geometry of the neutral. (a) Total ionization probability from numerical simulations including single ionization channel. (b) Angle-dependent factor $R(\theta_L)$ from the analytical analysis. Contributions from both Π_x and Π_y channels are included.

the outgoing flux removed by complex absorbing boundaries [22]. The Cartesian grid extended to ± 15 a.u. in all directions with a step size of 0.2 a.u. The analytical predictions are confirmed by the numerics, even though the details of the intensity dependence of the peak differ somewhat. The appearance of a local feature near $\theta_L = 0$ for stronger intensities is also present in both calculations.

The rotation of the maxima in the alignment-dependent rate is dictated by the maxima in the momentum-space representation of the orbital, located around 50°–60°. The momentum-space features become more important with increasing field strength. The interplay of coordinate and momentum-space features manifests itself via the contribution of the terms proportional to $F_{1,2,3}$, which arise from derivatives in the direction orthogonal to z and maximize near sharp coordinate-space features. Such sharp features correspond to higher momentum components.

While our current analysis leaves out such intriguing effects as the interplay of different orbitals (channels) in molecular ionization [23–25], which may become important in determining total strong-field ionization rates [13,25], the first steps towards extension to the multichannel case have already been done [25].

We thank Dr. O. Smirnova for stimulating discussions. M. Y. I. acknowledges support of Science and Innovation Grant No. EP/E036112/1 "Quantum Coherence." S. P. was partially supported by the Deutsche Forschungsgemeinschaft grant SM292/1-2.

*On leave from: National Research Council of Canada, 100 Sussex Drive, Ottawa, ON, K2A 0R6, Canada.

[1] See, e.g., Y. Huismans *et al.*, Science **331**, 61 (2010); M. Spanner *et al.*, J. Phys. B **37**, L243 (2004).
[2] L. Holmegaard *et al.*, Phys. Rev. Lett. **102**, 023001 (2009).
[3] M. Meckel *et al.*, Science **320**, 1478 (2008); H. Akagi *et al.*, Science **325**, 1364 (2009).
[4] F. H. M. Faisal, Theor. Chem. Acc. **127**, 175 (2009).
[5] X. M. Tong, Z. X. Zhao, and C. D. Lin, Phys. Rev. A **66**, 33402 (2002).
[6] A.-T. Le, R. R. Lucchese, and C. D. Lin, J. Phys. B **42**, 211001 (2009).
[7] S.-F. Zhao *et al.*, Phys. Rev. A **80**, 051402 (2009); **82**, 035402 (2010).
[8] G. A. Gallup and I. I. Fabrikant, Phys. Rev. A **81**, 033417 (2010); I. I. Fabrikant and G. A. Gallup, Phys. Rev. A **79**, 013406 (2009).
[9] D. Pavicic *et al.*, Phys. Rev. Lett. **98**, 243001 (2007).
[10] M. Abu-samha and L. B. Madsen, Phys. Rev. A **80**, 23401 (2009).
[11] M. Abu-samha and L. B. Madsen, Phys. Rev. A **81**, 033416 (2010).
[12] S. K. Son and Shih-I. Chu, Phys. Rev. A **80**, 011403(R) (2009).
[13] S. Petretti *et al.*, Phys. Rev. Lett. **104**, 223001 (2010).
[14] I. Thomann *et al.*, J. Phys. Chem. A **112**, 9382 (2008).
[15] J. Bertrand *et al.* (to be published).
[16] R. Murray, W. K. Liu, and M. Y. Ivanov, Phys. Rev. A **81**, 023413 (2010).
[17] V. S. Popov, Sov. Phys. Usp. **47**, 855 (2004), and references therein.
[18] A. A. Radzig and B. M. Smirnov, *Reference Data on Atoms, Molecules, and Ions* (Springer-Verlag, Berlin, 1985).
[19] S. Patchkovskii *et al.*, J. Chem. Phys. **126**, 114306 (2007).
[20] T. H. Dunning, Jr., J. Chem. Phys. **90**, 1007 (1989); R. A. Kendall, T. H. Dunning, Jr., and R. J. Harrison, J. Chem. Phys. **96**, 6796 (1992).
[21] M. Spanner and S. Patchkovskii, Phys. Rev. A **80**, 063411 (2009).
[22] D. E. Manolopoulos, J. Chem. Phys. **117**, 9552 (2002).
[23] O. Smirnova *et al.*, Nature (London) **460**, 972 (2009).
[24] Y. Mairesse *et al.*, Phys. Rev. Lett. **104**, 213601 (2010).
[25] Z. Walters and O. Smirnova, J. Phys. B **43**, 161002 (2010).